Nanoscale

Accepted Manuscript

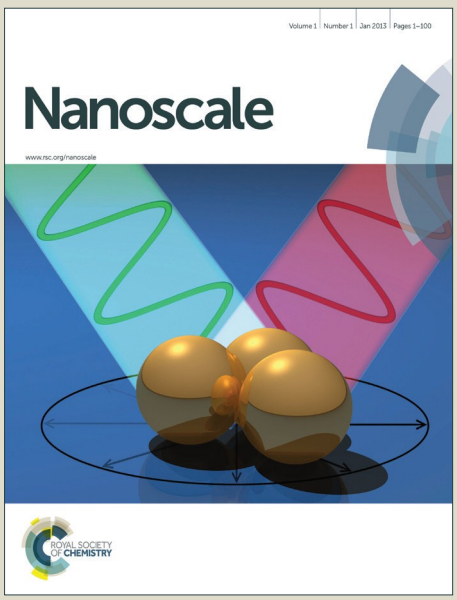

ROYAL SOCIETY OF CHEMISTRY

www.rsc.org/nanoscale

Promising Wet Chemical Strategies to Synthesize Cu Nanowires for Emerging Electronic Applications

D.V. Ravi Kumar[1], Kyoohee Woo[2,*], and Jooho Moon[1,*]

[1]*Department of Materials Science and Engineering, Yonsei University, 50 Yonsei-ro Seodaemun-gu, Seoul 120-749, Republic of Korea*

[2]*Advanced Manufacturing Systems Research Division, Korea Institute of Machinery and Materials, 156 Gajeongbuk-ro, Yuseong-gu, Daejeon 305-343, Republic of Korea*

Abstract

Copper nanowires (Cu NWs) are of particular interest for application as transparent and flexible conducting electrodes in 'see-through' and/or 'deformable' future electronics due to their excellent electrical, optical, and mechanical properties. It is necessary to develop reliable and facile methods to produce well-defined Cu NWs prior to their full exploitation. Among the wide variety of methods available to generate Cu NWs, solution-based synthesis routes are considered to be a promising strategy because of several advantages including fewer constraints on the selection of precursors, the solvent and reaction conditions, and the feasibility of large-scale low-cost production. Here, we provide a thorough review on various recently developed synthetic methodologies to obtain Cu NWs, with particular emphasis on wet chemical synthesis approaches including a hydrothermal route, reduction of metal precursors, and catalytic synthesis. The emerging applications of Cu NWs including transparent electrodes and flexible/stretchable electronics are also discussed, followed by brief comments on the remaining challenges and future research perspectives.

Keywords: Cu nanowires, wet chemical synthesis, flexible electrodes, transparent electrodes

[*]*E-mail: jmoon@yonsei.ac.kr; Fax: +82-2-312-5375; Tel: +82-2-2123-2855*

khwoo@kimm.re.kr; Fax: +82-42-868-7615; Tel: +82-42-868-7176

1. Introduction

In contrast to traditional opaque, rigid, and brittle electronics, future electronics that are required to be transparent, flexible, and even stretchable promise to lead to new and unconventional applications such as implantable conformal biosensors, wearable electronic devices, and highly deformable optoelectronic devices. For the realization of these devices, transparent and deformable conducting electrodes are demanded. Consequently, various conducting materials such as conducting polymers,[1-3] carbon nanotubes,[4-11] and graphene[12-14] as well as metal nanostructures[15-22] have been extensively researched as alternatives to conventional brittle conducting materials (e.g., indium tin oxide, ITO). Conducting polymers including poly(3,4-ethylenedioxythiophene):poly(styrenesulfonate) (PEDOT:PSS) are long-standing alternatives that offer the ability to be printed from solution as well as mechanical flexibility. However, in spite of their good processability, they suffer from a relative high sheet resistance and poor stability. It is feasible to use carbon-based nanomaterials such as graphene due to their flexibility and stretchability, but they also suffer from relatively poor conductivity and difficulty in scalable production with high material costs. Among the candidates, metal nanowires (NWs) are considered as one of the most promising materials for flexible and transparent electrodes. Metals are the most conductive materials on earth due to their high free-electron density. In addition, in the form of NWs with very small diameters (smaller than visible wavelengths) and long lengths, they can be highly transparent and flexible while maintaining a good electrical conductivity. Because of the many abovementioned advantages, Ag NWs have recently been utilized in several applications with limited performance in flexible and transparent electrodes.[23-38] However, in spite of their successful demonstration, practical applications of Ag NWs are still limited because of their scarcity and high cost.[39-45] Compared to Ag, Cu is cheaper and more

abundant, resulting in dramatically lower NW costs. Therefore, a facile synthesis approach that allows the production of high-quality copper nanowires (Cu NWs) in large quantities is in great demand.

Various methodologies have been reported to synthesize Cu NWs including chemical vapor deposition,[46-47] vacuum thermal decomposition,[48] electro-spinning process,[49-51] and soft or hard template-based methods.[52-55] Chemical vapor deposition of Cu NWs generally involves the vaporization of organometallic copper precursors as well as the deposition and condensation of vapors on a solid substrate in a controlled atmosphere, which is beneficial to fabricate highly aligned, vertically grown NWs on a substrate. However, this process often suffers from extremely restrained conditions including high temperatures, very low pressures, and large-scale production. These problems can be addressed by using a vacuum thermal decomposition method. Recently, the Cui group suggested that, by combination of electrospinning and electro-less deposition, junction-free Cu NWs networks could be fabricated at ambient temperature and pressure, allowing fabrication of highly conductive NW films even on plastic substrates. However, this method consisting of complicated multi-steps needs to be simplified for practical use, even though electrospinning of polymeric nanofibers is a well-established field. Template-based methods using hard templates (e.g., an anodized aluminum oxide, AAO) or soft templates (e.g., deoxyribonucleic acid, DNA) can also be used to fabricate Cu NWs. These methods are effective in controlling the morphologies of nanowires within the confines of the templates used in the synthesis, but there are some drawbacks related to the template removal and scale-up to the gram scale.

Recently, wet chemical methods including hydrothermal synthesis, reduction of metal precursors, and catalytic synthesis are being considered promising strategies for the synthesis of

Cu NWs due to several advantages including fewer constraints regarding the selection of precursors, solvent, and reaction conditions as well as the feasibility of large-scale production. As a result, wet chemical methods have been extensively explored to fabricate Cu NWs. However, to the best of our knowledge, there are few reports of a comprehensive discussion of the various wet chemical routes. Therefore, we introduce the various wet chemical approaches utilized to generate Cu NWs and compare their pros and cons. In addition, we summarize the experimental procedures, growth mechanisms, and morphological features of the NWs synthesized by each method. Concurrently, the factors that can affect the yield, properties, and quality of the products are also covered. In addition, the use of Cu NWs in various existing applications such as transparent electrodes, deformable conductors, and sensors is reviewed. Finally, we briefly outline the remaining challenges and possible future research perspectives.

2. Wet Chemical Synthesis of Cu Nanowires

2.1 Hydrothermal methods

The hydrothermal method can be considered as one of the widely used wet chemical approaches to synthesize Cu NWs. This process is generally carried out under elevated temperatures and pressures using an apparatus consisting of a steel pressure vessel that can withstand high temperatures and pressures known as an autoclave. One of the first reports of the hydrothermal synthesis of Cu NWs was based on the reduction of a Cu(II)-glycerol complex in high concentration NaOH and glycerol aqueous solutions with the assistance of sodium dodecyl benzenesulfonate (SDBS) surfactant.[56] The reaction was performed at 120 °C for 20 h and Cu NWs with an average diameter of ~85 nm and lengths of few tens of micrometers could be successfully synthesized. By observing that only very irregular, aggregated copper nanoparticles

were formed in the absence of surfactant, they suggested that the surfactant prevents the aggregation of Cu seeds formed in the initial stages of the reaction and kinetically controls the growth rate of various crystallographic facets of FCC Cu to attain anisotropy. In addition, they determined that the relatively high concentrations of NaOH and glycerol in the reaction mixture, which led to increased viscosity of the mixture, were favorable for the formation of the Cu NWs in a high yield. They explained that the high viscosity suppresses the aggregation of copper particles.

In 2005, Shi *et al.* synthesized Cu NWs by a hydrothermal reaction using a simpler chemical solution.[57] The reaction solution was prepared by adding only copper chloride ($CuCl_2$) and octadecylamine (ODA) in a water solvent followed by heating at 120-180 °C for 48 h. They observed that with only ODA, copper(II) cations could be completely reduced to elemental copper at a temperature of ~120 °C to obtain ultra-long Cu NWs with uniform diameters of 30-50 nm and lengths of several millimeters (aspect ratio > 10^5). This observation indicates that ODA can play multiple roles in the formation of Cu NWs, serving as both a soft reducing agent and a capping agent. At a higher reaction temperature (160-180 °C), the diameters of the Cu NWs increased due to a higher reduction rate and the crystallinity of the Cu NWs improved via thermodynamic diffusion.

Instead of the ODA surfactant, hexadecylamine (HDA)[58] or tetradecylamine (TDA)[59] can be used to synthesize Cu NWs. With these surfactants, glucose as a reducing agent is generally added in the reaction solution. In this case, the hydrothermal reaction is conducted at 120-130 °C in a relatively shorter time (< ~10 h) and Cu NWs with diameters of 40-60 nm and lengths of a few hundred micrometers are produced. The molar ratio of glucose to the copper precursor is an important factor to be controlled because the number of copper seeds depends

significantly on the concentration of the reducing agent. For example, as the molar ratio of glucose to the copper precursor was increased from 1:1 to 4:1, copper nanoparticles were formed instead of NWs because a large number of copper seeds instantaneously developed with the high concentration of the reducing agent and they had a strong tendency to aggregate as larger nanoparticles, as shown in Fig. 1. Moreover, by using various copper precursors such as copper chloride ($CuCl_2$), copper nitride ($Cu(NO_3)_2$), copper acetate ($C_4H_6CuO_4$), and cupric bromide ($CuBr_2$), final copper products could be formed with many different shapes including nanowires, nanoparticles, hollow spheres, and nanoflakes. From these results, it was concluded that the different activities of various copper-amine complexes created from the reaction between the copper precursor and surfactant could affect the growth rate, resulting in different shapes of the final products.

Cu NWs can also be synthesized by an environmentally benign hydrothermal route using non-toxic ascorbic acid (i.e., Vitamin C) without the involvement of linear alkyl amines such as HDA, TDA, and ODA.[60] However, as explained above, linear alkyl amines were used in most reports of hydrothermal routes to synthesize Cu NWs. This indicates that they play important roles in the formation of Cu NWs such as SDBS suggested by Liu *et al*. The roles of alkyl amines in the synthesis of Cu NWs were systematically studied by Kumar *et al*.[61] They observed that Cu NWs were not formed when both cetyltrimethylammonium bromide (CTAB) and polyvinylpyrrolidone (PVP), which are known to stabilize penta-twinned seeds, were used as substitutes for alkyl amines.[55] In addition, pencil-like pentagonal rods with micron-sized widths were formed when the amount of alkyl amines was not sufficient. Based on these observations, they proposed important dual roles of alkyl amines in the formation of the Cu NWs, as visualized in Fig. 2. In the initial stages of the reaction, alkyl amines act as a complexing agent to form a

suitable metal-amine complex for the self-seed generation. Slow reduction of this metal-amine complex allows for the generation of twinned seeds which are later grown into NWs by consuming newly generated seeds. In the latter stages of the reaction, the alkyl amines play an additional role as a capping agent by selective adsorption on newly generated seeds, allowing them to grow into NWs.

Recently, Pan and co-workers presented a facile hydrothermal approach to synthesize a large amount of Cu NWs by using a commercial electric pressure cooker (Fig. 3a).[62] Oleylamine (OLA) and oleic acid were employed as dual surfactants to enhance the dispersion stability of Cu NWs and glucose was used as the reducing agent. 4 liters of the reaction solution was prepared by mixing the aqueous solution of glucose and copper chloride with an ethanol solution of the dual surfactants. The reaction was conducted at a temperature of 116 °C for 12 h. Finally, they obtained Cu NWs with an average diameter of 45 nm and lengths of 60-90 μm while obtaining a quantity of grams (over ~2 g) in a batch, as shown in Fig. 3b and 3c. In addition, they showed that the hydrophobic NWs capped with OLA and oleic acid could be altered to hydrophilic NWs capped with PVP by a ligand exchange process. Consequently, the Cu NWs could be well dispersed in a polar solvent such as ethanol.

2.2 Reduction of copper precursors

Cu NWs can also be synthesized by reducing copper ions at atmospheric pressure. We classify this method into three categories based on the type of reducing agent used in the synthesis: oleylamine (OLA)-based method, glucose-assisted approach, and hydrazine-assisted approach.

2.2.1 Oleylamine-based approach

It is well known that OLA, which is a liquid at room temperature, can act as a solvent and a reducing agent as well as a capping agent. Moreover, it can form a copper-amine complex with the copper precursor (copper(I) chloride (CuCl)). Consequently, additional additives for reduction, complexation, and NW capping are unnecessary in this technique. The reaction tends to be performed at slightly higher temperatures (170-200 °C) than hydrothermal methods. Ye *et al*. successfully synthesized Cu NWs with diameters of approximately 50 nm (Fig. 4a and 4b) and lengths >10 μm using this approach.[63] They explained that the formation of Cu NWs is based on the disproportionation of Cu^{I} (Fig. 4c), which involves the initial dissolution of CuCl through coordination with OLA and the subsequent disproportionation of Cu^{1+} complexes into Cu^{2+} and Cu^{0} at 200 °C. In addition, it was also found that the stability of OLA-coated Cu NWs against oxidation can be enhanced by surface ligand exchange with trioctylphosphine (TOP). Yang *et al*. conducted a comprehensive mechanistic study of the reaction of copper(I) chloride with OLA that produces Cu NWs and proposed a self-seeded process as the growth mechanism of the Cu NWs.[64] In the initial stage of the reactions, five-twinned copper seeds are formed by homogeneous nucleation. As the reaction proceeds, OLA preferentially adsorbs on the {100} facets of the growing seeds. Thereafter, copper atoms generated by an Ostwald ripening process or reduction reaction of a copper-amine complex continue to deposit and crystallize on the relatively poor capped {111} facets, leading to the formation of NWs.

2.2.2 Glucose-assisted approach

It was reported that long Cu NWs can be synthesized at a low temperature of 100 °C for 6 h under atmospheric pressure.[65] Similar to the hydrothermal method, glucose and HDA were employed as a reducing agent and a capping agent, respectively, in a copper chloride aqueous solution. The synthesized NWs have diameters of ~24 ± 4 nm and lengths ranging from several

tens to hundreds of micrometers. By using inductively-coupled plasma mass spectrometry (ICP-MS) and scanning electron microscopy, it was found that the Cu precursors were almost completely converted into atomic Cu and Cu NWs were obtained in high yield without any purification process. In this approach, depending on the concentrations of HDA and glucose, the products are also developed with various shapes, as shown in Fig. 5. For example, when the concentration of glucose is high, the decahedral seeds formed in the early stage favor isotropic growth due to the fast reduction. As the reaction proceeds further, glucose is consumed, resulting in lower reduction rates and then, the isotropic growth can be switched to an anisotropic mode, leading to the formation of pentagonal bipyramids or tadpole-like nanowires (Fig. 5a). As identified in the hydrothermal approach, these observations also suggest that the amounts of glucose and HDA play important roles in controlling the final morphology of Cu nanocrystals.

2.2.3 Hydrazine-assisted approach

A hydrazine-assisted reduction method to produce Cu NWs was initially reported by Chang *et al.*[66] In this method, Cu NWs could be produced by the reduction of Cu^{2+} in the presence of hydrazine as a strong reducing agent and ethylenediamine (EDA) as a capping agent in an aqueous solution of sodium hydroxide (NaOH). The formation of metallic copper is based on the following redox reaction under basic conditions.

$$2Cu^{2+} + N_2H_4 + 4OH^- \rightarrow 2Cu + N_2 + 4H_2O$$

The reaction was conducted at a temperature of 60 °C for 60 min and the synthesized NWs were reported to have diameters of 90-120 nm with an aspect ratio of more than 350. It is noted that the hydrazine reduction method can facilitate the formation of Cu NWs at a shorter time (< 1 h) and lower temperature (< 80 °C) compared to other methods used to produce Cu NWs, although a highly toxic hydrazine solvent is used. In this method, a high concentration of NaOH is

essential to prevent copper ions from forming copper hydroxide precipitates. Also, the interplay between NaOH and EDA was recognized where in the case of a high concentration of NaOH, a small amount of EDA is needed, while for a lower concentration of NaOH, an increased amount of EDA is required in order to obtain high regularity for the one-dimensional NW products. This hydrazine-based reduction route was further modified to demonstrate its potential for large-scale production.[67] For the reaction scaled up by a factor of 200 (from 0.006 to 1.2 g of Cu NWs), NaOH (2,000 mL, 15M), $Cu(NO_3)_2$ (100 mL, 0.2M), EDA (30 mL), and hydrazine (2.5 mL, 35 wt%) were added to a reaction flask and heated to 80 °C for 60 minutes. The color of the solution changed from a royal blue (Fig. 6a) to a reddish brown color (Fig. 6b), indicating that Cu NWs were formed by the reduction of Cu^{2+} ions. NWs with diameters of 90 ± 10 nm and lengths of 10 ± 3 μm were synthesized, as shown in Fig. 6c.

Several growth mechanisms of Cu NWs in the hydrazine-based reduction method have been suggested. Rathmell *et al*. unprecedentedly observed spherical copper particles at the end of most synthesized NWs (Fig. 6c) and based on the characterization of the time-dependent morphologies of the NWs, discovered that the wires grow from single crystalline spherical seeds.[67] The selected area electron diffraction (SAED) pattern of the nanowires indicated that the Cu NWs consisted of a single-crystalline domain and grew via atomic addition to {110} planes, which have the highest surface energy among the low-index facets of FCC copper metal. As another growth mechanism of Cu NWs, axial screw dislocation-driven growth was also suggested by Meng *et al*.[68] The presence of axial screw dislocations along the ⟨110⟩ direction and Eshelby twists associated with the dislocations was suggested to be proof that the Cu NWs form by a dislocation-driven mechanism. In addition, they postulated a dual role of OH^- ions in the reaction in which the OH^- ions not only provide a suitable pH environment for the redox

reaction, but also undergo complexation with Cu^{2+} to form $[Cu(OH)_4]^{2-}$. They believed that the activity of Cu^{2+} ions could be lowered by this complexation and dislocation driven growth could be promoted.

Recently, in a hydrazine-based solution reduction route, seed-mediated growth was suggested as a new mechanism which accounts for the role of Cu_2O seeds and EDA, as illustrated in Fig. 7.[69] In the presence of a sufficient amount of EDA, a small amount of Cu_2O nanoparticles generated from reaction (1) aggregates to form the seeds and subsequently, they are reduced to form metallic Cu aggregates by reaction (2). Finally, Cu aggregates grow to Cu NWs via reduction of the ionic copper precursor based on reaction (3).

$$4[Cu(OH)_4]^{2-} + N_2H_4\ (aq) \rightarrow 2Cu_2O(s) + N_2\ (g) + 6H_2O + 8OH^- \quad (1)$$

$$2Cu_2O(s) + N_2H_4\ (aq) \rightarrow 4Cu(s) + N_2\ (g) + 2H_2O \quad (2)$$

$$4[Cu(OH)_4]^{2-} + N_2H_4\ (aq) \rightarrow 4Cu(s) + N_2\ (g) + 4OH^- + 4H_2O \quad (3)$$

On the other hand, removal of EDA from the reaction solution leads to the rapid formation of Cu_2O octahedra. When these octahedra are reintroduced as seeds in the reaction solution, Cu NWs can grow out from them with a high yield, verifying the mechanism that accounts for the role of Cu_2O seeds in the copper nanowire growth. In addition, the dimension of the NWs can be simply controlled by varying the concentration of the seed solution in the reaction solution for the NW growth.

Hydrazine reduction was utilized for the production of Cu NWs in a high yield via a continuous flow solvothermal reduction process using a non-aqueous solvent.[70] The feed precursor solution for typical synthesis of Cu NWs is prepared by dissolving $CuCl_2 \cdot 2H_2O$ and PVP in an ethanol solvent. Then, the precursor solution is injected into a continuous flow reactor (CFR) under refluxing conditions at 80 °C using a peristaltic pump with a separately prepared,

mixed solution of hydrazine monohydrate ($N_2H_4 \cdot H_2O$) and ethanol, as shown in Fig. 8. The reaction to form Cu NWs is based on the reduction of Cu^{2+} ions by the hydrazine monohydrate and the synthesized NWs have diameters in the range of 60-110 nm and the lengths of over several tens of micrometers. It has sometimes been reported in other studies that Cu NWs could not be formed when the synthesis is conducted in the presence of only PVP surfactant because it could not form a suitable copper complex to generate penta-twinned seeds.[54] However, interestingly, in this study, PVP was used as the sole capping agent/surfactant for the growth of Cu NWs. This result indicates that PVP can be also absorbed onto the specific facet {100} of the seed particles, leading to the anisotropic growth of Cu NWs. However, further studies are required to understand the roles of PVP in the growth of NWs.

2.3 Catalytic methods

Zhang *et al*. reported the catalytic mediated synthesis of Cu NWs in liquid crystalline medium of binary HDA and CTAB surfactants.[71] The synthesized NWs are well-dispersed and ultralong (several tens micrometers to several millimeters). The procedure for the synthesis of Cu NWs involves a non-aqueous protocol, in which Cu acetylacetonate ($Cu(acac)_2$) is added to the liquid crystalline medium, formed by melting HDA and CTAB at an elevated temperature of 180 °C. A silicon wafer sputtered with catalytic platinum (Pt) is placed into the mixtures and then they are kept at 180 °C for 10 h, leading to the spontaneous formation of Cu NWs. The proposed formation mechanism is depicted in Fig. 9. First, a medium with a tubular liquid-crystalline structure was provided by the melted amphiphilic CTAB and HDA mixture. As the added Cu precursor molecules rapidly coordinate with HDA and Br^- from CTAB, tubular channels are enriched with the metal moieties. Subsequently, HDA reduces the metal moieties, forming metal

clusters and building particles within the tubular channels. Because of the preferential adsorption of HDA and Br^- on the {200} planes, confined growth of the building clusters and particles leads to the formation of Cu nanowires along the ⟨110⟩ direction. The change of the ratio between HDA and CTAB in the reaction medium can alter their assembled structure from micelles to rods to a more complicated liquid-crystalline structure, accordingly leading to the formation of various shapes of Cu products. The yield of NWs can be improved by using Pt nanoparticles with diameters of 5 nm as a catalyst instead of a Pt-sputtered Si wafer.[72] Pt nanoparticles in the reaction medium facilitates electron transfer from reducing moieties (NH^{4+}) to Cu^{2+} ions and also works as the seeds for heterogeneous nucleation of Cu atoms.

Similarly, Cu NWs with a high aspect ratio (diameter of 16.2 ± 2 nm and lengths up to 40 μm) were synthesized using a nickel(II) acetylacetone ($Ni(acac)_2$) catalyst in an OLA solution.[73] The mechanism is described in Fig. 10. Firstly, Ni^{2+} ions are transformed to Ni^0 atoms under heating at 175 °C. Then, Cu nanosrystals can be formed by the galvanic replacement reaction between Ni^0 and Cu ions in OLA. These Cu nanocrystals as seeds slowly grow to NWs in the presence of Cl^- ions resulting from the $CuCl_2$ precursor. In this study, it was suggested that the Cl^- ions from the $CuCl_2$ precursor are indispensable because Cl^- would attach onto the {100} facets and lead to strongly anisotropic growth. In a very similar way, Guo *et al*. successfully synthesized Cu nanocubes and nanowires.[74] It was also observed in this study that Cl^- ions which bond to the surface of the Cu crystal seeds play a major role in controlling the morphology. Interestingly, the final morphology (cube or wire) depends on whether TOP is added to the reaction solution. In the presence of TOP, the reduction rate of Ni^{2+} is very slow due to the formation of TOP-Ni^{2+} coordination complexes, leading to the generation of single-crystal seeds at the initial stage, which finally grow into nanocubes. However, in the absence of TOP, rapid

reduction from Ni^{2+} into Ni^0 occurs, resulting in the formation of multi-twined crystal seeds that finally develop into NWs.

Table 1 summarizes the features of the various wet chemical methods discussed above. The hydrothermal route is a very promising and reproducible method to synthesize highly crystalline, thin Cu NWs with a wide range of lengths from sub-micrometers to several millimeters. In addition, the feasibility to synthesize Cu NWs on the large scale (grams) has been experimentally demonstrated. However, because it generally requires a vessel that can withstand high temperatures and pressures, the production cost for the scale up can be greatly increased. Furthermore, this route suffers from a long reaction time (several hours to several days) and high temperature (120-180 °C). In the OLA-based reduction approach, any additional additives for reduction, complexation, and NW capping are not included because OLA can act as the solvent, reducing agent, and capping agent. However, the reaction tends to be performed at a high temperature (170-200 °C) for a long time of more than 6 h. The glucose-assisted reduction route is a kind of modified hydrothermal method using glucose and HDA. Although a long reaction time is required, it is conducted at a relatively low temperature of 100 ^{o}C under atmospheric pressure. Cu NWs synthesized by this method are very thin (diameter of ~20 nm) and long (several tens to hundreds of micrometers). The hydrazine reduction method is appropriate for the formation of Cu NWs in a short reaction time (< 1 h) at a low temperature (< 80 °C), which is also capable of producing Cu NWs in large quantities. However, the length of the Cu NWs synthesized by the hydrazine reduction route is limited to a few tens of micrometers. In addition, the large amount of toxic and explosive hydrazine solvent required for the mass production of Cu NWs has to be resolved to address safety concerns. Compared to OLA- or glucose- or hydrazine-based reduction methods, catalytic methods seem to be favorable for the fabrication of ultra-long

nanowires, but they require a long time (4-10 h) and high temperature (170-180 ^{o}C) for the reaction. In addition, a cost effective metal catalyst needs to be explored.

3. Applications of Copper NWs

3.1. Transparent conducting electrodes (TCEs)

3.1.1. Properties of Cu NW based TCEs

TCEs are essential components of various optoelectronic devices such as flexible solar cells, touch screens, and displays. Cu NWs with their excellent optical transparency, electrical conductivity, and economic feasibility have been identified as a promising material for TCEs. Therefore, many researchers have attempted to develop Cu NWs-based TCEs to surpass the transparency and conductivity of other currently used TCEs.

Wiley and co-workers conducted a number of studies focused on the development of TCEs by using a Cu NW-dispersed solution.[67] They used NWs with lengths of 10 ± 3 μm and diameters of 90 ± 10 nm synthesized by a hydrazine reduction method and fabricated transparent conductive electrodes by attaching the polycarbonate membrane which filters out the Cu NWs on glue-coated sticky film and peeling it away. The optical transmittance (T) and sheet resistance (Rs) of the prepared TCEs were determined to be 67% and 61 Ω/sq, respectively. To address the performance degradation resulting from the poor dispersibility and restricted dimensions (low aspect ratio) of the NWs, they further modified the synthesis method. Reaction mixture was heated at 80 °C for a very short time (about 3 min) and PVP was then quickly added to the reaction mixture before cooling and, thereby well-dispersed long (l > 20 μm) and thin (d = 60 nm) NWs could be obtained.[75] Cu NW based transparent films were successfully fabricated by Meyer rod coating as a promising, scalable coating method (Fig. 11a and 11b). With the

purpose of removing organics and welding contacting nanowires, the prepared films were placed in plasma cleaner for 15 min under a forming gas atmosphere (95 % nitrogen and 5% hydrogen) and then heated to 175 °C in a tube furnace with a pure hydrogen atmosphere. The fabricated Cu NW-based TCEs exhibited enhanced performance in terms of transparency (T = 85%) and conductivity (Rs = 30 Ω/sq) and the bent film can easily carry enough current to power the LED, as seen in Fig. 11c. This is because well dispersed long NWs can form a more effective electron percolation network with a lower NW number density than aggregated short NWs. In addition, little change (30 Ω/sq to 40 Ω/sq) of the sheet resistance of Cu NW films was observed after 1,000 cycles of compressive and tensile bending from a radius of curvature of 10 mm to a radius of curvature of 2.5 mm whereas the sheet resistance of ITO films increased by a factor of 400 after just 250 bends (Fig. 11d). Until recently, many researchers have attempted to synthesize Cu NWs with excellent dispersibility and a high aspect ratio (> 1,000) for high performance applications (T > 90%, Rs <100 Ω/sq), comparable to the properties of ITO and Ag NWs.

3.1.2. Prevention of Cu oxidation

Protecting Cu NWs from oxidation is a critical issue to be addressed for the practical implementation of Cu NWs-based transparent conducting films because copper is prone to oxidation when exposed to oxygen under ambient conditions. To prevent oxidation of the Cu NWs, Rathmell et al. reported solution phase synthesis of Ni-coated Cu NWs (inset in Fig. 12) via reducing Ni ions on the surface of Cu NWs with hydrazine (N_2H_4).[76] Coating copper NWs with Ni resulted in small losses of transmittance and conductivity due to the enlarged diameter of the NWs and intrinsically higher resistivity of Ni, but it greatly improved their resistance to oxidation. As seen in Fig. 12, the sheet resistance of the bare Cu NW-based TCEs began to increase after 1 day in a dry oven at 85 °C and soared by an order of magnitude after 5 days. The

sheet resistance of Ag NW films increased by an order of magnitude after 13 days. In comparison, the sheet resistance of the Ni-coated Cu NW-based TCEs remained remarkably stable over a period of 30 days. Instead of nickel, transparent metal oxide or graphene was also applied to the shell of the Cu NWs and the shells can prevent oxidation of Cu NWs without degradation of the transmittance and conductivity.[45,77] In addition, recently, several researchers have attempted to cover up pre-made Cu NW films with materials such as reduced graphene oxide (RG-O) or Al-doped ZnO (AZO).[78-79] The cover layers of RG-O and AZO can not only protect the Cu NWs underneath it from oxidation, but also provide 2-dimensional pathways for charge transfer between non-percolated NWs, resulting in high stability and high conductivity.

On the other hand, annealing process to reduce the junction contact resistance between Cu NWs is typically required to be performed in carefully controlled atmosphere (an inert-gas or vacuum environment) because Cu NWs can be rapidly oxidized upon the thermal annealing process in air. Such a controlled atmosphere-based annealing can result in a considerable increase in production cost and time and, in turn hinder the wider use of Cu NWs for transparent conductors. To solve this problem, a plasmonic nanowelding process using a polarized laser was employed for the fabrication of Cu-NW percolation network based transparent conductor.[80] It was confirmed that the oxidation of Cu NWs was dramatically suppressed even under ambient conditions due to the localized heating at the NW junction with rapid laser scanning (< 100 μs). Recently, it was also found that by using focused laser beam, photothermochemical reduction of Cu_xO NW to Cu NW could be induced rapidly at room temperature under ambient condition without using any vacuum or inert gas environment.[81] Interestingly, as this laser photoreduction process is reversible, Cu_xO NW can be turned back into Cu NW repetitively. It indicates that oxidized Cu_xO NW can be recycled as conductive electrodes. As an another solution, the

chemical treatment using acetic acid or lactic acid has been also developed for reducing the contact resistance between Cu NWs.[79,82] By simply adding acids into the solution containing NWs or dipping NW-coated sample in acids at room temperature, the passivating oxide/hydroxide and organic moieties on the surface of Cu NWs can be effectively removed, allowing direct contact between the NWs.

3.1.3. Device integration

It has been demonstrated that Cu NW-based TCEs could be successfully integrated in practical applications such as solar cells and OLED. Won *et al*. successfully implemented transparent AZO/Cu NW/AZO composite electrodes into a $Cu(In_{1-X},Ga_X)(S,Se)_2$ (CIGSSe) thin-film solar cell which exhibited a power conversion efficiency of 7.1% (Fig. 13a).[79] The transparent AZO/Cu NW/AZO composite electrode exhibited a high transparency (83.9% at 550 nm) and low sheet resistance (35.9 Ω/sq) at room temperature whereas the thermal stability and oxidation resistance of the TCEs were dramatically improved due to the AZO layer fully covering the Cu NWs. Recently, a graphene shell-coated Cu NWs-based TCE was applied to a bulk heterojunction polymer solar cell (Fig. 13b). It was observed that encapsulation of the Cu NWs with gas impermeable graphene shells improved the thermal oxidation and chemical stability of the TCE. The fabricated polymer solar cell exhibited a power conversion efficiency of 4.04% with an open-circuit voltage (V_{OC}) of 0.73 V, a short circuit current density (J_{SC}) of 8.20 mA/cm^2, and a fill factor (FF) of 67.8%.[45] In addition, a flexible OLED has been also demonstrated using a Cu NW TCE that is monolithically embedded on the surface of a transparent glass-fabric reinforced (GFRHybrimer) plastic film.[83] The CuNW-GFRHybrimer film exhibited excellent opto-electrical performance (Rs = 25 Ω/sq and T = 82%).

3.2 Deformable conductors

Cu NWs are stable, excellent electrically conductive, and highly deformable conductors. Tang *et al*. reported a low-cost, simple yet efficient strategy to fabricate ultralight aerogel monoliths and conducting rubber ambers from Cu NWs (Fig. 14).[84] To form a Cu NW-PVA composite aerogel, they froze the mixing solution of Cu NWs and poly(vinyl alcohol) (PVA) and then freeze-dried it. In this method, PVA is essential to stabilize the Cu NW scaffolds and enhance the mechanical robustness and flexibility of the aerogels. The Cu NW-PVA aerogels (Fig. 14b) could be embedded into a polydimethylsiloxane (PDMS) matrix and the resulting Cu NW-PVA-PDMS conductors (Fig. 14c) were manufactured into arbitrary 1D (plaited fibers), 2D (twisted sheets), and 3D (triangular prism) shapes by simple cutting, as shown in Fig. 14a, d-f. Won *et al*. also fabricated Cu NWs-based deformable electrodes.[85] They transferred the NWs onto a pre-strained PDMS substrate, leading to excellent operation of the electrodes even under a tensile strain greater than 100% and reversible stretching properties after 130 cycles. For further enhancement of the stretchability, they introduced a reversible and extremely stretchable (up to 700% of strain) helical Cu NW-based conducting spring. As shown in Fig. 15a, as a template, a screw was inserted into a straw with a slightly larger diameter and the PDMS precursor liquid then infiltrated the gap between the screw and the straw. After curing, a helical-shaped PDMS substrate was obtained and the Cu NW network was then transferred onto this substrate and finally, the helix-shaped Cu NW conductor was fabricated. This helical conductor exhibited an unprecedented stretchability of 700% with a relative resistance change of only 3.9, which is superior compared to other results (inset in Fig. 15b) reported in the literature for highly stretchable electrodes. At the same time, this helical-structured Cu NW conductor showed stable and reversible stretchability during repeated stretching cycles at a tensile strain of 100%.

Recently, it was found that laser nanowelded Cu NWs based conductor could be stretchable enough to endure large strain (>250%) with no substantial cracks. In the case of laser nanowelded Cu-NW network, unintended cracks could be prevented due to firmly-welded junctions of the NWs. This indicates the laser annealing can be effective in improving stretchability of metal NW random network based electrodes.

3.3 Sensors

Electrochemical non-enzymatic glucose sensors with high sensitivity and a low detection limit have been explored because the monitoring of glucose in the blood and cells of the human body is of paramount importance in the diagnosis and treatment of diabetes.[86-87] For these sensors, Cu-based materials have been recently widely investigated because they not only show excellent electrocatalytic activity for glucose oxidation, but also have advantages including low cost and a high electrical conductivity. In particular, one-dimensional Cu-based NWs are of great interest in the development of electrochemical biosensors due to their efficient electron transfer along the 1-D direction and good mechanical strength.

Zhang *et al*. developed a glucose sensor based on Cu NWs with an average diameter of 150 nm and an average length of 30 μm synthesized by a hydrazine reduction method.[88] The developed glucose sensor was able to detect glucose with a limit of detection as low as 35 nM, a wide linear range, and high sensitivity, which can be attributed to the good catalytic ability, large surface area, excellent conductivity, and efficient electron transfer of the Cu NWs. It was observed that interference from uric acid, ascorbic acid, acetaminophen, fructose, and sucrose at the physiological concentrations is insignificant, indicating that the sensor has excellent selectivity for glucose. It was confirmed that the prepared glucose sensor has good accuracy and

high precision for the quantification of the glucose concentration in human serum samples. Recently, Huang *et al*. also developed a Cu NWs-CNT hybrid non-enzymatic biosensor using hydrothermally synthesized Cu NWs where the average diameter of the Cu NWs was about 50 nm with lengths of several micrometers.[89] The sensor exhibited excellent sensitivity, a low detection limit of 0.26 μM, high stability, and rapid response (< 1 s) over a wide linear concentration range up to 3 mM. These results imply that Cu NWs are a desirable candidate in the development of sensitive and selective non-enzymatic glucose sensors.

4. Conclusions and Future Prospects

Cu NWs have garnered great interest as promising next generation conducting electrodes due to their high conductivity, mechanical flexibility, and cost effectiveness. As a result, ongoing efforts to develop a facile approach that allows the production of high-quality copper nanowires (Cu NWs) in large quantities and their utilization in various electronic applications are being carried out. Among the various methods developed so far, we mainly focused on wet chemical approaches including a hydrothermal route, the reduction of metal precursors, and a catalytic method, which are considered to be facile, scalable strategies to produce Cu NWs. For each technique, the growth mechanisms, properties of the Cu NWs, and key factors to determine the yield or quality of the products were discussed in detailed and several important applications of Cu NWs were also highlighted. From this review, we hope that the readers will understand the product features and underlying formation mechanism of each method.

Despite the significant scientific advancements in the syntheses and applications of Cu NWs, there are still limitations in transferring the lab scale achievements to the industrial scale. Various issues such as inefficient processes with a long reaction time and the use of toxic solvents or high cost catalysts need to be addressed. Concurrently, continuing efforts are required

to overcome the inherent surface oxidation of Cu NWs and facilitate controllability of the NW dimensions, large-scale production on the kilogram scale, and adaptability to roll-to-roll based scalable and cost effective coating and patterning techniques before they can be widely used on the industrial scale. Furthermore, the widespread practical implementation of Cu NWs can be accelerated in conjunction with developing new device concepts and integrated architectures. Such investigations may advance the realization of future electronics that can be transparent, flexible, and even stretchable.

Acknowledgements

This work was supported by a National Research Foundation (NRF) of Korea grant funded by the Korean government (MSIP) (No. 2012R1A3A2026417). This work was also partially supported by the National Research Council of Science & Technology (OD1300).

References

1. M. Vosgueritchian, D. J. Lipomi and Z. Bao, *Adv. Funct. Mater.*, 2012, **22**, 421-428.
2. S. Kirchmeyer and K. Reuter, *J. Mater. Chem.*, 2005, **15**, 2077-2088.
3. N. Kim, S. Kee, S. H. Lee, B. H. Lee, Y. H. Kahng, Y. Jo, B. Kim and K. Lee, *Adv. Mater.*, 2014, **26**, 2268-2272.
4. Z. Wu, Z. Chen, X. Du, J. M. Logan, J. Sippel, M. Nikolou, K. Kamaras, J. R. Reynolds, D. B. Tanner, A. F. Hebard and A. G. Rinzler, *Science*, 2004, **305**, 1273–1276.
5. C. Yu, C. Masarapu, J. Rong, B. Wei and H. Jiang, *Adv. Mater.*, 2009, **21**, 4793.
6. T. Yamada, Y. Hayamizu, Y. Yamamoto, Y. Yomogida, A. Izadi-Najafabadi, D. N. Futaba and K. Hata, *Nat. Nanotechnol.*, 2011, **6**, 296-301.
7. Z. Yu, X. Niu, Z. Liu and Q. Pei, *Adv. Mater.*, 2011, **23**, 3989-3994.
8. D. Zhang, K. Ryu, X. Liu, E. Polikarpov, J. Ly, M. E. Tompson and C. Zhou, *Nano Lett.*, 2006, **6**, 1880-1886.
9. C. Yu, C. Masarapu, J. Rong, B. Wei and H. Jiang, *Adv. Mater.*, 2009, **21**, 4793-4797.
10. H. Z. Geng, K. K. Kim, K. P. So, Y. S. Lee, Y. Chang and Y. H. Lee, *J. Am. Chem. Soc.*, 2007, **129**, 7758.
11. S. Park, M. Vosguerichian and Z. Bao, *Nanoscale*, 2013, **5**, 1727-1752.
12. K. S. Kim, Y. Zhao, H. Jang, S. Y. Lee, J. M. Kim, K. S. Kim, J. Ahn, P. Kim, J. Choi and B. H. Hong, *Nature*, 2009, **457**, 706-710.
13. G. Eda, G. Fanchini and M. Chhowalla, *Nat. Nanotechnol.*, 2008, **3**, 270-274.
14. T. Gao, Z. Li, P. Huang, G. J. Shenoy, D. Parobek, S. Tan, J. Lee, H. Liu and P. W. Leu, *ACS Nano*, 2015, **9**, 5440-5446.
15. L. B. Hu, H. Wu and Y. Cui, *Mater. Res. Soc. Bull.*, 2011, **36**, 760-765.
16. P. Lee, J. Lee, H. Lee, J. Yeo, S. Hong, K. H. Nam, D. Lee, S. S. Lee and S. H. Ko, *Adv. Mater.*, 2012, **24**, 3326-3332.
17. S. De, T. M. Higgins, P. E. Lyons, E. M. Doherty, P. N. Nirmalraj, W. J. Blau, J. J. Boland and J. N. Coleman, *ACS Nano*, 2009, **3**, 1767-1774.
18. S. Nam, M. Song, D. Kim, B. Cho, H. M. Lee, J. Kwon, S. Park, K. Nam, Y. Jeong, S. Kwon, Y. C. Park, S. Jin, J. Kang, S. Jo and C. S. Kim, *Sci. Rep.*, 2014, **4**, 4788.
19. D. C. Hyun, M. Park, C. Park, B. Kim, Y. Xia, J. H. Hur, J. M. Kim, J. J. Park and U. Jeong, *Adv. Mater.*, 2011, **23**, 2946-2950.
20. L. Hu, H. S. Kim, J. Y. Lee, P. Peumans and Y. Cui, *ACS Nano*, 2010, **4**, 2955-2963.
21. X. Y. Zeng, Q. K. Zhang, R. M. Yu and C. Z. Lu, *Adv. Mater.*, 2010, **22**, 4484-4488.
22. M. Shin, J. H. Song, G. Lim, B. Lim, J. Park and U. Jeong, *Adv. Mater.*, 2014, **26**, 3706-3711.
23. S. M. Bergin, Y. Chen, A. R. Rathmell, P. Charbonneau, Z. Lib and B. J. Wiley, *Nanoscale*, 2012, **4**, 1996.
24. D. A. Dinh, K. N. Hui, K. S. Hui, P. Kumar and J. Singh, *Rev. Adv. Sci. Eng.*, 2013, **2**, 1-22.
25. S. Yao and Y. Zhu, *Nanoscale*, 2014, **6**, 2345.
26. H. Cheong, R. E. Triambulo, G. Lee, I. Yi and J. Park, *ACS Appl. Mater. Inter.*, 2014, **6**, 7846-7855.
27. K. Zilberberg, F. Gasse, R. Pagui, A. Polywka, A. Behrendt, S. Trost, R. Heiderhoff, P. Görrn and T. Riedl, *Adv. Funct. Mater.*, 2014, **24**, 1671-1678.
28. M. Lee, K. Lee, S. Kim, H. Lee, J. Park, K. Choi, H. Kim, D. Kim, D. Lee, S. Nam and J. Park, *Nano Lett.*, 2013, **13**, 2814-2821.
29. Y. Cheng, R. Wang, J. Sun and L. Gao, *ACS Nano*, 2015, **9**, 3887-3895.

30. S. Choi, J. Park, W. Hyun, J. Kim, J. Kim, Y. B. Lee, C. Song, H. J. Hwang, J. H. Kim, T. Hyeon and D. Kim, *ACS Nano*, 2015, **9**, 6626-6633.
31. J. Lee, P. Lee, H. Lee, D. Lee, S. S. Lee and S. H. Ko, *Nanoscale*, 2012, **4**, 6408.
32. P. Lee, J. Ham, J. Lee, S. Hong, S. Han, Y. D. Suh, S. E. Lee, J. Yeo, S. S. Lee, D. Lee and S. H. Ko, *Adv. Funct. Mater.*, 2014, **24**, 5671–5678.
33. S. Hong, H. Lee, J. Lee, J. Kwon, S. Han, Y. D. Suh, H. Cho, J. Shin, J. Yeo and S. H. Ko, *Adv. Mater.*, 2015, **27**, 4744–4751.
34. S. Hong, J. Yeo, J. Lee, H. Lee, P. Lee, S. S. Lee and S. H. Ko, *J. Nanosci. Nanotechnol.*, 2015, **15**, 2317-2323.
35. J. Lee, P. Lee, H. B. Lee, S. Hong, I. Lee, J. Yeo, S. S. Lee, T. Kim, D. Lee and S. H. Ko, *Adv. Funct. Mater.*, 2013, **23**, 4171–4176.
36. K. K. Kim, S. Hong, H. M. Cho, J. Lee, Y. D. Suh, J. Ham and S. H. Ko, *Nano Lett.*, 2015, **15**, 5240−5247.
37. I. Chang, T. Park, J. Lee, H. B. Lee, S. Ji, M. H. Lee, S. H. Ko, S. W. Cha, *Int. J. Hydrogen Energy*, 2014, **39**, 7422 -7427.
38. I. Chang, T. Park, J. Lee, M. H. Lee, S. H. Ko and S. W. Cha, J. Mater. Chem. A, 2013, **1**, 8541-8546.
39. S. Ye, A. R. Rathmell, I. E. Stewart, Y. Ha, A. R. Wilson, Z. Chena and B. J. Wiley, *Chem. Commun.*, 2014, **50**, 2562.
40. M. Kevin, G. Y. R. Limb and G. W. Ho, *Green Chem.*, 2015, **17**, 1120-1126.
41. Z. Yin, C. Lee, S. Cho, J. Yoo, Y. Piao and Y. S. Kim, *small*, 2014, **10**, 5047-5052.
42. S. Bhanushali, P. Ghosh, A. Ganesh and W. Cheng, *small*, 2015, **11**, 1232-1252.
43. C. Sachse, N. Weiß, N. Gaponik, L. Müller-Meskamp, A. Eychmüller and K. Leo, *Adv. Energy Mater.*, 2014, **4**, 1300737.
44. W. Hu, R. Wang, Y. Luc and Q. Pei, *J. Mater. Chem. C*, 2014, **2**, 1298.
45. Y. Ahn, Y. Jeong, D. Lee and Y. Lee, *ACS Nano*, 2015, **9**, 3125-3133.
46. H. Choi and S. Park, *J. Am. Chem. Soc.*, 2004, **126**, 6248-6249.
47. C. Kim, W. Gu, M. Briceno, I. M. Robertson, H. Choi and K. Kim, *Adv. Mater.*, 2008, **20**, 1859-1863.
48. D. Haase, S. Hampel, A. Leonhardt, J. Thomas, N. Mattern and B. Büchner, *Surf. Coat. Technol.*, 2007, **201**, 9184-9188.
49. A. Khalil, R. Hashaikeh and M. Jouiad, *J. Mater. Sci.*, 2014, **49**, 3052-3065.
50. H. Wu, L. Hu, M. W. Rowell, D. Kong, J. J. Cha, J. R. McDonough, J. Zhu, Y. Yang, M. D. McGehee and Y. Cui, *Nano Lett.*, 2010, **10**, 4242-4248.
51. P. Hsu, D. Kong, S. Wang, H. Wang, A. J. Welch, H. Wu and Yi Cui, *J. Am. Chem. Soc.*, 2014, **136**, 10593−10596.
52. R. Inguanta, S. Piazza and C. Sunseri, *Appl. Surf. Sci.*, 2009, **255**, 8816-8823.
53. G. A. Gelves, Z. T. M. Murakami, M. J. Krantz and J. A. Haber, *J. Mater. Chem.*, 2006, **16**, 3075-3083.
54. J. Pate, F. Zamora, S. M. D. Watson, N. G. Wright, B. R. Horrocks and A. Houlton, *J. Mater. Chem. C*, 2014, **2**, 9265.
55. C. F. Monson and A. T. Woolley, *Nano Lett.*, 2003, **3**, 359-363.
56. Z. Liu, Y. Yang, J. Liang, Z. Hu, S. Li, S. Peng and Y. Qian, *J. Phys. Chem. B*, 2003, **107**, 12658-12661.
57. Y. Shi, H. Li, L. Chen and X. Huang, *Sci. Technol. Adv. Mater.*, 2005, **6**, 761-765.
58. M. Mohl, P. Pusztai, A. Kukovecz and Z. Konya, *Langmuir*, 2010, **26**, 16496-16502.

59. B. Jia, M. Qin, Z. Zhang, A. Chu, L. Zhang, Y. Liu and X. Qu, *J. Mater. Sci.*, 2013, **48**, 4073-4080.
60. W. Wang, G. Li and Z. Zhang, *J. Cryst. Growth*, 2007, **299**, 158-164.
61. D. V. Ravi Kumar, I. Kim, Z. Zhong, K. Kim, D. Lee and J. Moon, *Phys. Chem. Chem. Phys.*, 2014, **16**, 22107.
62. S. Li, Y. Chen, L. Huang and D. Pan, *Inorg. Chem.*, 2014, **53**, 4440-4444.
63. E. Ye, S. Zhang, S. Liu and M. Han, *Chem. Eur. J.*, 2011, **17**, 3074-3077.
64. H. Yang, S. He and H. Tuan, *Langmuir*, 2014, **30**, 602-610.
65. M. Jin, G. He, H. Zhang, J. Zeng, Z. Xie and Y. Xia, *Angew. Chem. Int. Ed.*, 2011, **50**, 10560-10564.
66. Y. Chang, M. L. Lye and H. C. Zeng, *Langmuir*, 2005, **21**, 3746-3748.
67. A. R. Rathmell, S. M. Bergin, Y. Hua, Z. Li and B. J. Wiley, *Adv. Mater.*, 2010, **22**, 3558-3563.
68. F. Meng and S. Jin, *Nano Lett.*, 2012, **12**, 234-239.
69. S. Ye, A. R. Rathmell, Y. Ha, A. R. Wilson and B. J. Wiley, *small*, 2014, **10**, 1771-1778.
70. Y. Zhao, Y. Zhang, Y. Li, Z. Hec and Z. Yan, *RSC Adv.*, 2012, **2**, 11544-11551.
71. D. Zhang, R. Wang, M. Wen, D. Weng, X. Cui, J. Sun, H. Li and Y. Lu, *J. Am. Chem. Soc.*, 2012, **134**, 14283-14286.
72. Y. Cheng, S. Wang, R. Wang, J. Sun and L. Gao, *J. Mater. Chem. C*, 2014, **2**, 5309.
73. H. Guo, N. Lin, Y. Chen, Z. Wang, Q. Xie, T. Zheng, N. Gao, S. Li, J. Kang, D. Cai and D. Peng, *Sci. Rep.*, 2013, **3**, 2323.
74. H. Guo, Y. Chen, H. Ping, J. Jin and D. Peng, *Nanoscale*, 2013, **5**, 2394.
75. A. R. Rathmell and B. J. Wiley, *Adv. Mater.*, 2011, **23**, 4798-4803.
76. A. R. Rathmell, M. Nguyen, M. Chi and B. J. Wiley, *Nano Lett.*, 2012, **12**, 3193-3199.
77. Z. Chen, S. Ye, I. E. Stewart and B. J. Wiley, *ACS Nano*, 2014, **8**, 9673-9679.
78. I. N. Kholmanov, S. H. Domingues, H. Chou, X. Wang, C. Tan, J. Kim, H. Li, R. Piner, A. J. G. Zarbin and R. S. Ruoff, *ACS Nano*, 2013, **7**, 1811-1816.
79. Y. Won, A. Kim, D. Lee, W. Yang, K. Woo, S. Jeong and J. Moon, *NPG Asia Mater.*, 2014, **6**, e105.
80. S. Han, S. Hong, J. Ham, J. Yeo, J. Lee, B. Kang , P. Lee, J. Kwon, S. S. Lee, M. Yang and S. H. Ko, *Adv. Mater.,* 2014, **26**, 5808–5814.
81. S. Han, S. Hong, J. Yeo, D. Kim, B. Kang, M. Yang and S. H. Ko, *Adv. Mater.* 2015, DOI: 10.1002/adma.201503244
82. I. E. Stewart, A. R. Rathmell, L. Yan, S. Ye, P. F. Flowers, W. You and B. J. Wiley, *Nanoscale*, 2014, **6**, 5980.
83. H. Im, S. Jung, J. Jin, D. Lee, J. Lee, D. Lee, J. Lee, I. Kim and B. Bae, *ACS Nano*, 2014, **8**, 10973-10979.
84. Y. Tang, S. Gong, Y. Chen, L. W. Yap and W. Cheng, *ACS Nano*, 2014, **8**, 5707-5714.
85. Y. Won, A. Kim, W. Yang, S. Jeong and J. Moon, *NPG Asia Mater.*, 2014, **6**, e132.
86. P. Si, Y. Huang, T. Wang and J. Ma, *RSC Adv.*, 2013, 3, 3487-3502.
87. G. Wang, X. He, L. Wang, A. Gu, Y. Huang, B. Fang, B. Geng and X. Zhang, *Microchim. Acta*, 2013, **180**, 161-186.
88. Y. Zhang, L. Su, D. Manuzzi, H. V. E. de los Monteros, W. Jia, D. Huo, C. Hou, Y. Lei, *Biosens. Bioelectron.*, 2012, **31**, 426-432.
89. J. Huang, Z. Dong, Y. Li, J. Li, J. Wang, H. Yang, S. Li, S. Guo, J. Jin, R. Li, *Sens. Actuat. B-Chem.*, 2013, **182**, 618-624.

Table 1. Summary of wet chemical methods used to produce Cu NWs.

Method	Reaction Conditions	Properties of Cu NWs	Merits & demerits	Ref.
Hydrothermal synthesis	Reaction temperature From 120 °C to 200 °C	Diameter From 30 nm to 60 nm	Merits - It is very promising and reproducible for the synthesis of highly crystalline NWs. - It is less constrained by the solubility of the precursors. - An environmentally benign capping agent such as ascorbic acid is available. - It was experimentally demonstrated to be feasible for large scale production on the gram scale.	56-62
	Reaction time From several hours to several days	Length From a few tens to several millimeters	Demerits - It generally requires a long reaction time. - It requires a vessel that can withstand high reaction temperatures and pressures, leading to increased production costs for scale up.	
OLA-based reduction route	Reaction temperature From 170 °C to 200 °C	Diameter From 50 nm to 80 nm	Merits - Additional additives for reducing copper ions and capping of NWs are not necessary because OLA can act as a solvent, reducing agent, and capping agent.	63-64
	Reaction time From several hours to several days	Length Few tens of micrometers	Demerits - It generally requires a long reaction time. - The length of the NWs is limited to a few tens of microns. - It requires time-consuming heating protocols aimed at facilitating the dissolution of precursors.	

Glucose-assisted reduction route	Reaction temperature 100 °C	Diameter From 20 nm to 30 nm	Merits - It is carried out at low temperatures under atmospheric condition. - It is suitable for the synthesis of very thin and long NWs.	65
	Reaction time From several hours to several days	Length From several tens of micrometers to several hundreds of micrometers	Demerits - It generally requires a long reaction time, like the hydrothermal method.	
Hydrazine-assisted reduction route	Reaction temperature From 60 °C to 80 °C	Diameter From 90 nm to 120 nm	Merits - The reaction temperatures and reaction times are low compared to other wet chemical methods. - It can be used to synthesize large quantities of Cu NWs.	66-70
	Reaction time From 15 min to 120 min	Length Few tens of micrometers	Demerits: - The length of the NWs is limited to a few tens of microns. - The use of small amount of highly toxic and explosive hydrazine could not pose an issue in the case of small scale synthesis of Cu NWs. However, more quantity of hydrazine required for the large scale synthesis could be harmful.	
Catalysis method	Reaction temperature From 170 °C to 180 °C	Diameter From 15 nm to 70 nm	Merits: - It is relatively convenient to control the dimension of Cu NWs. - The reaction time is relatively short, compared to most wet chemical methods	71-74
	Reaction time 10 hours	Length From several tens of micrometers to several millimeters	Demerits: - An expensive catalyst such as Pt is used. - It is generally conducted at a high temperature.	

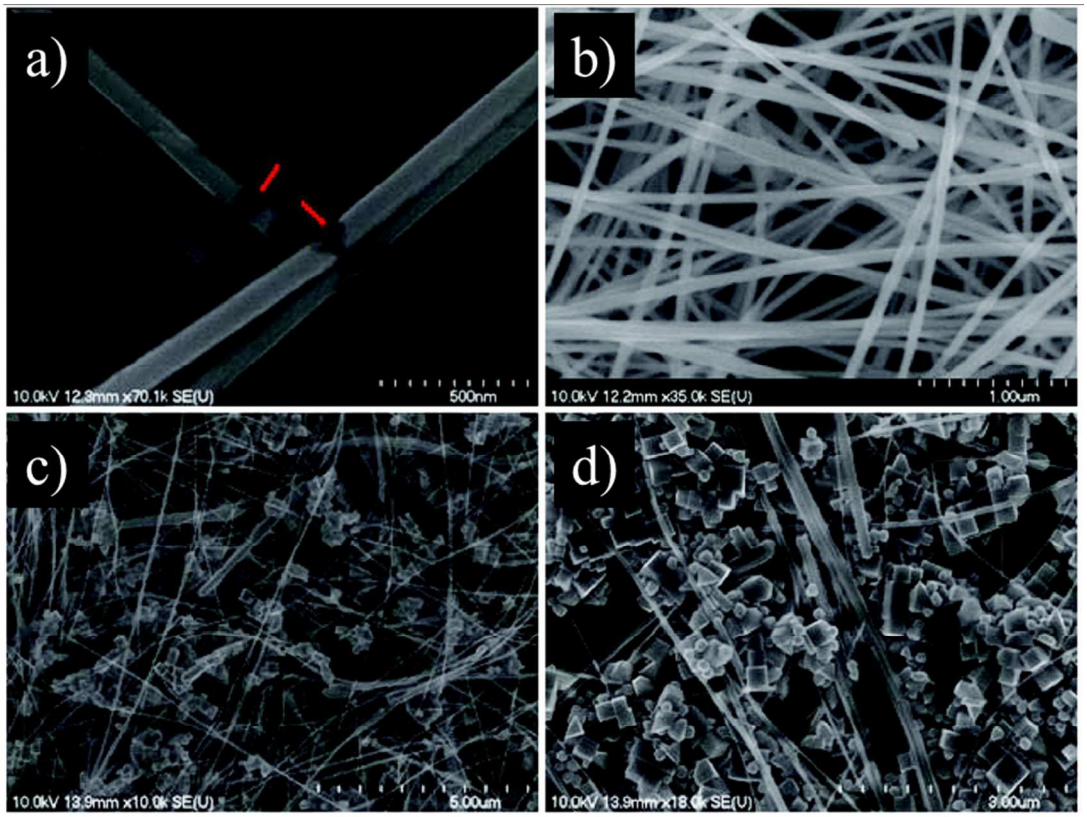

Figure 1. SEM images of Cu NWs hydrothermally synthesized with the following glucose/copper salt ratios: a) 0.2:1, b) 1:1, c) 3:1, and d) 4:1. Reproduced with permission from ref. 58. Copyright 2010, American Chemical Society.

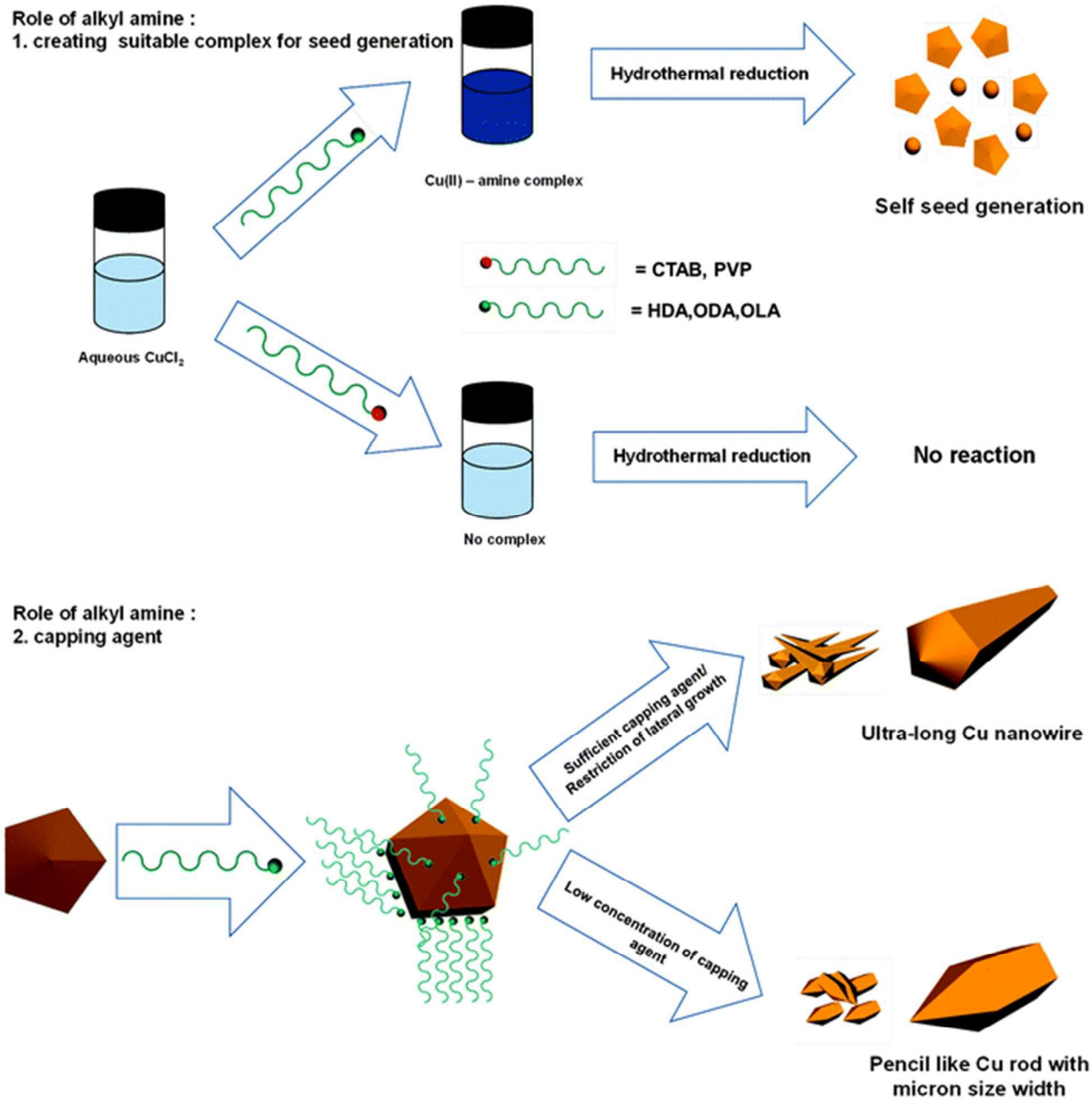

Figure 2. Schematic representation of the dual role of alkyl amines in the synthesis of Cu NWs. Reproduced with permission from ref. 61. Copyright 2014, Royal Society of Chemistry.

Figure 3. Photographs of the a) commercial pressure cooker used for the hydrothermal synthesis, b) 4 liters of the Cu NW solution, and c) SEM image of Cu NWs. Reproduced with permission from ref. 62. Copyright 2014, American Chemical Society.

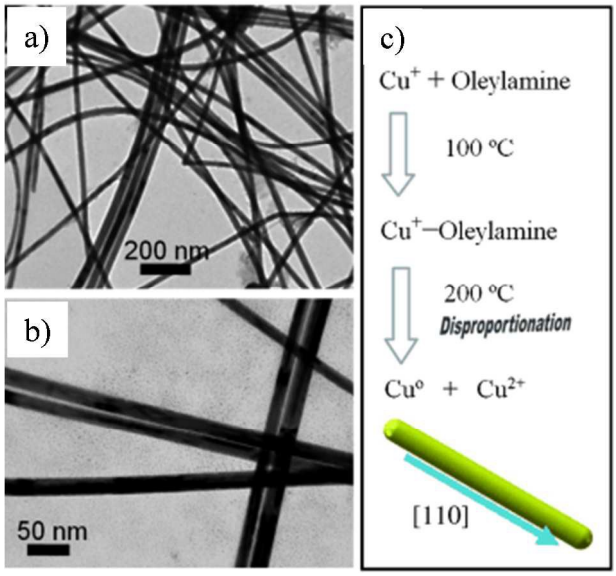

Figure 4. Anisotropic growth of Cu NWs by the disproportional reaction of CuCl in an OLA-based reduction approach. a) Low-magnification TEM image and b) magnified TEM image of Cu NWs. c) Schematic disproportional reaction for the formation of Cu NWs. Reproduced with permission from ref. 63. Copyright 2011, Wiley-VCH.

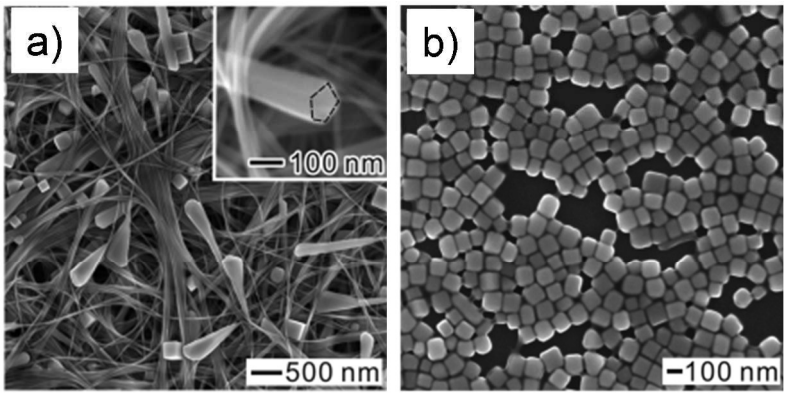

Figure 5. SEM images of a) tadpole-like Cu NWs and b) Cu nanocubes synthesized by a glucose-based reduction route. The change of the shapes is dependent on the concentrations of HDA and glucose. Reproduced with permission from ref. 65. Copyright 2011, Wiley-VCH.

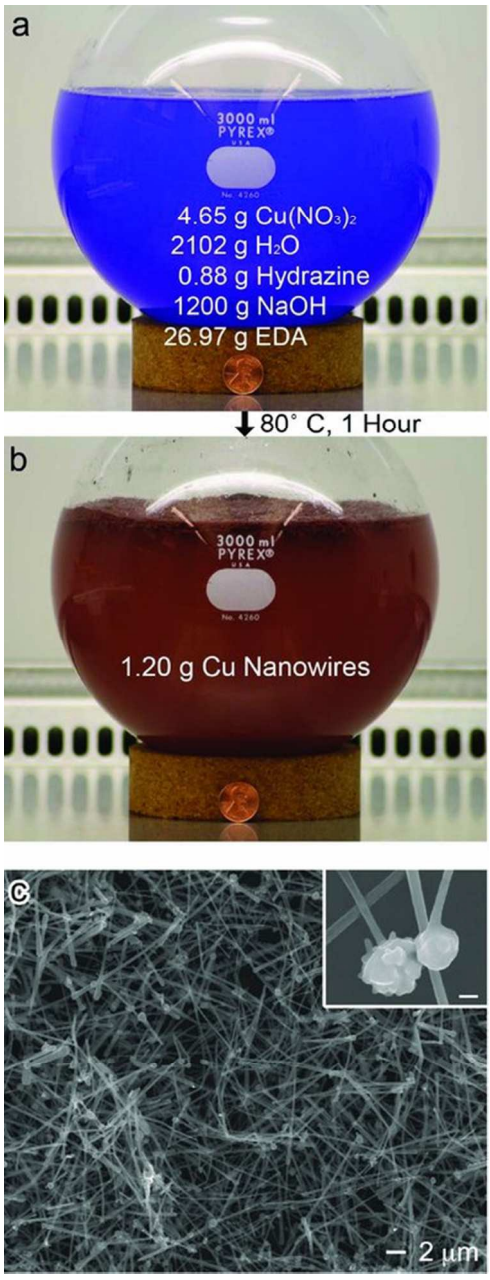

Figure 6. Photographs of the reaction flask a) before and b) after the synthesis at 80 °C for 1 hr. c) SEM image of Cu NWs. The nanowires have diameters of 90 ± 10 nm and lengths of 10 ± 3 µm. The inset shows Cu NWs with spherical copper particles attached at one end (scale bar = 200 nm). Reproduced with permission from ref. 67. Copyright 2010, Wiley-VCH.

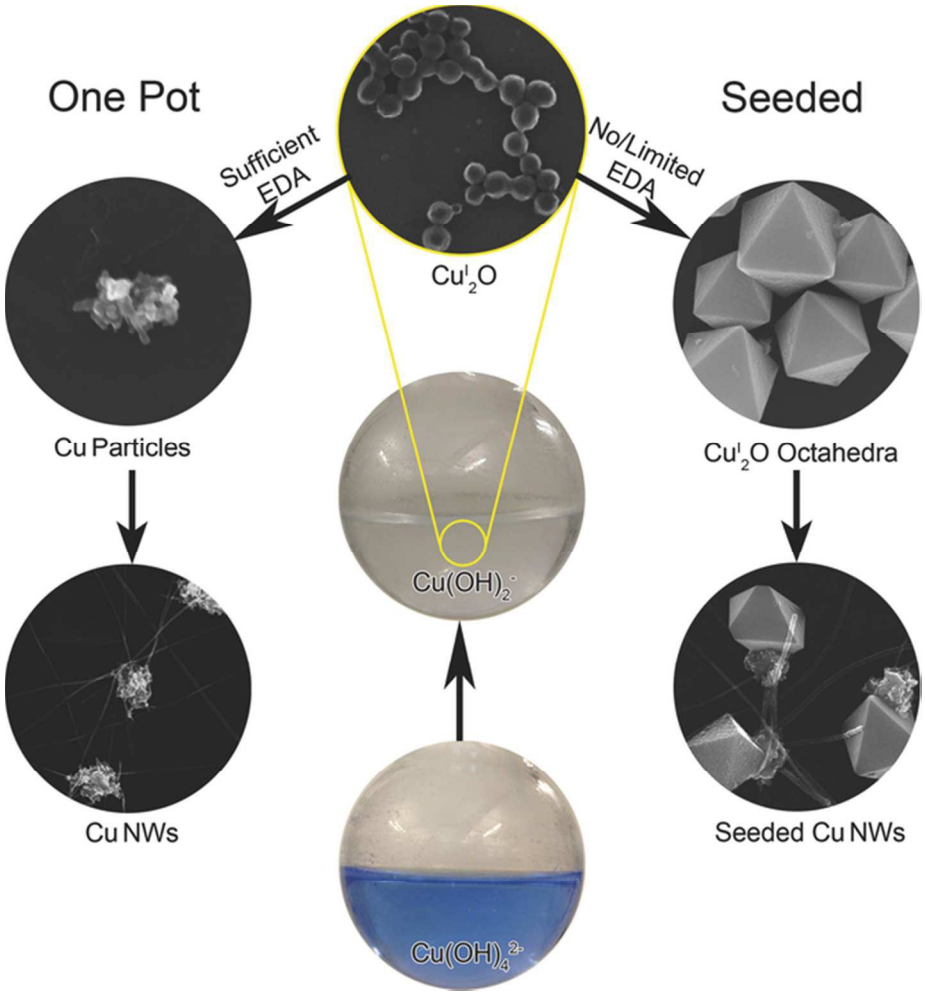

Figure 7. Schematic representation for the EDA-dependent reaction pathways in the hydrazine-based approach. Reproduced with permission from ref. 69. Copyright 2014, Wiley-VCH.

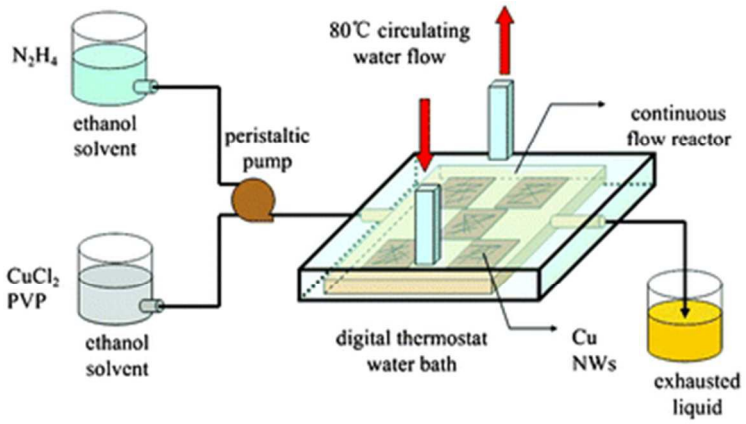

Figure 8. Schematic of the CFR for Cu NW growth. Reproduced with permission from ref. 70. Copyright 2012, Royal Society of Chemistry.

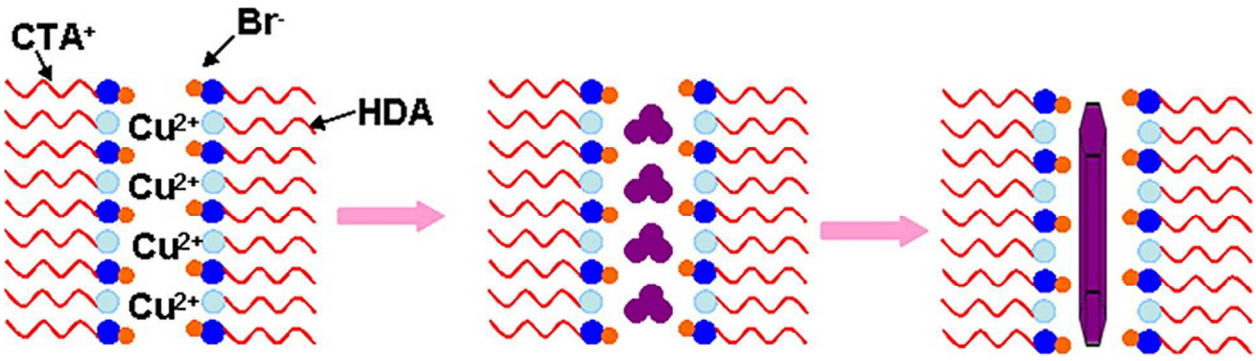

Figure 9. Schematic representation of the formation of Cu NWs directed by liquid crystalline medium. Reproduced with permission from ref. 71. Copyright 2012, American Chemical Society.

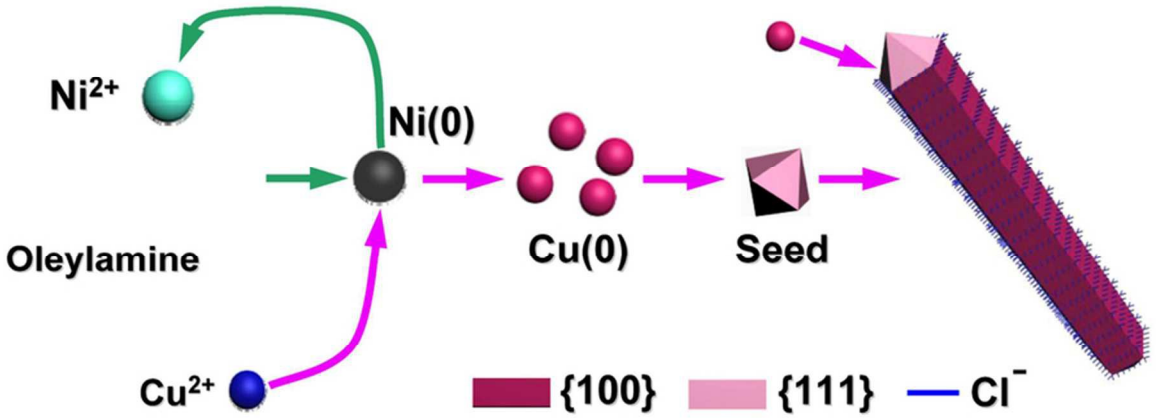

Figure 10. Schematic of the formation mechanism of Cu NWs in the presence of a nickel(II) acetylacetone ($Ni(acac)_2$) catalyst in the OLA solution. The Ni^{2+} and Cl^- ions play critical roles in promoting the growth of high aspect ratio Cu NWs. Reproduced with permission from ref. 73. Copyright 2013, Nature Publishing Group.

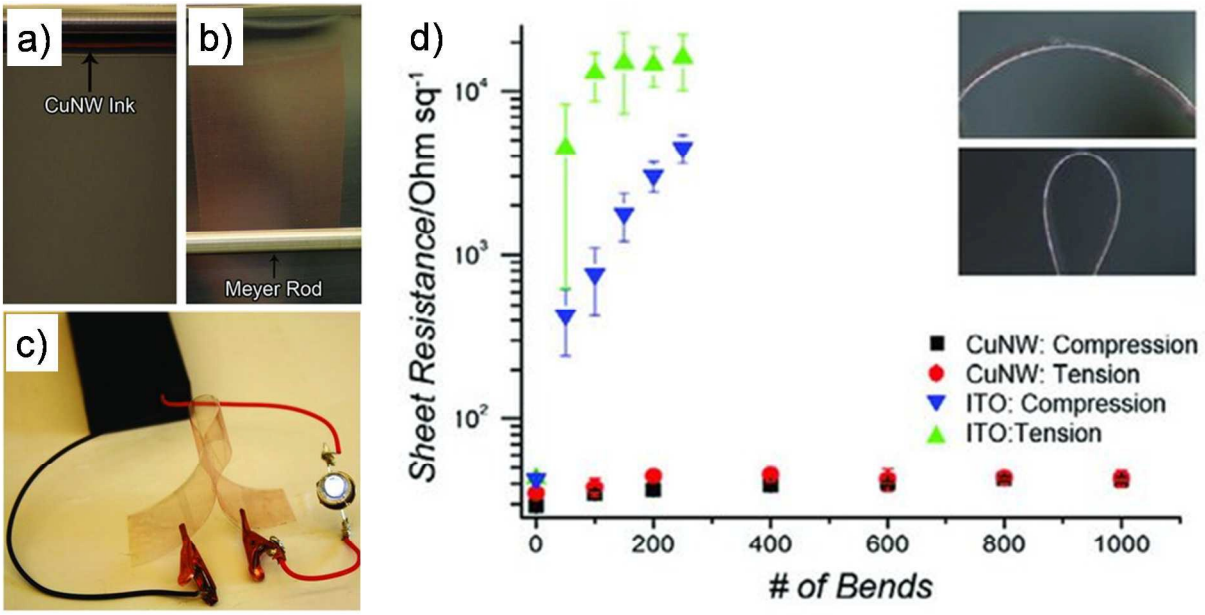

Figure 11. Cu NW ink a) before and b) after coating on PET with a Meyer rod. c) A bent Cu NW film completing an electrical circuit with a battery pack and a LED. d) Plot of the sheet resistance versus the number of bends for Cu NW films (85% transparent) and ITO on PET. The inset shows the radius of curvature before (10 mm) and after bending (2.5 mm). Reproduced with permission from ref. 75. Copyright 2011, Wiley-VCH.

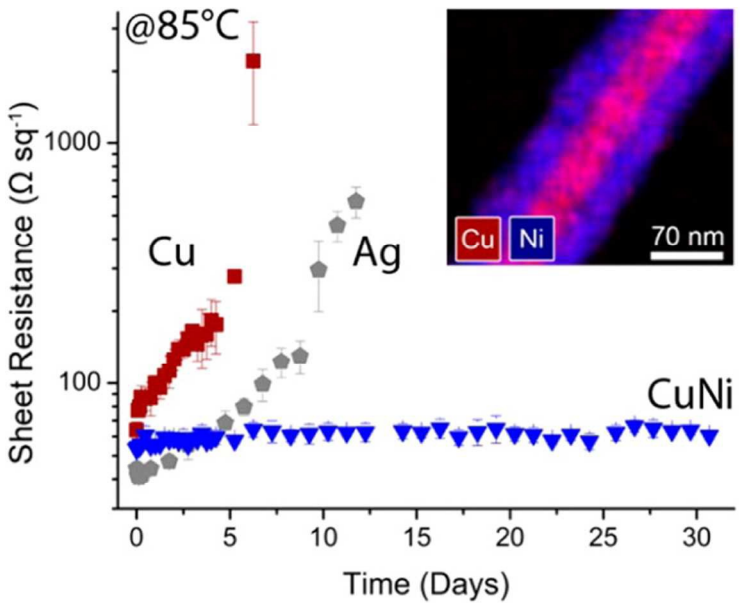

Figure 12. Plot of the sheet resistance vs. time for films of Ag NWs, Cu NWs, and Ni-coated Cu NWs stored at 85°C. The inset shows energy dispersive X-ray spectroscopy images of Ni-coated Cu NWs. Reproduced with permission from ref. 76. Copyright 2012, American Chemical Society.

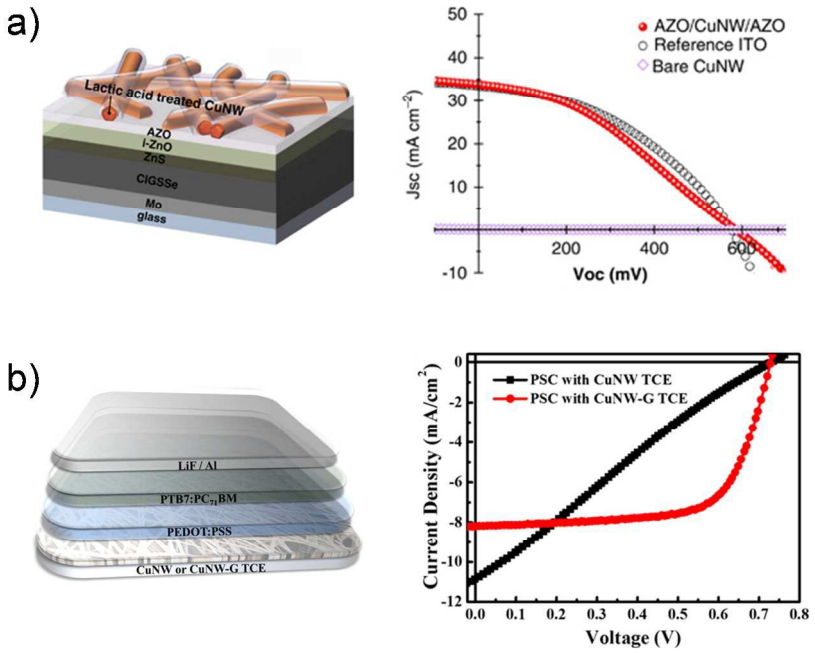

Figure 13. a) Schematic of the structure of a CIGSSe thin-film solar cell using an AZO/Cu NW/AZO composite electrode and I–V characteristics of ITO single film, bare Cu NW film, and AZO/Cu NW/AZO composite electrode-incorporated CIGSSe thin-film solar cells. Reproduced with permission from ref. 79. Copyright 2014, Nature Publishing Group. b) Device architecture of bulk heterojunction polymer solar cells using Cu NW or Cu NW-G TCE and the I–V characteristics of the corresponding cells. Reproduced with permission from ref. 45. Copyright 2015 American Chemical Society.

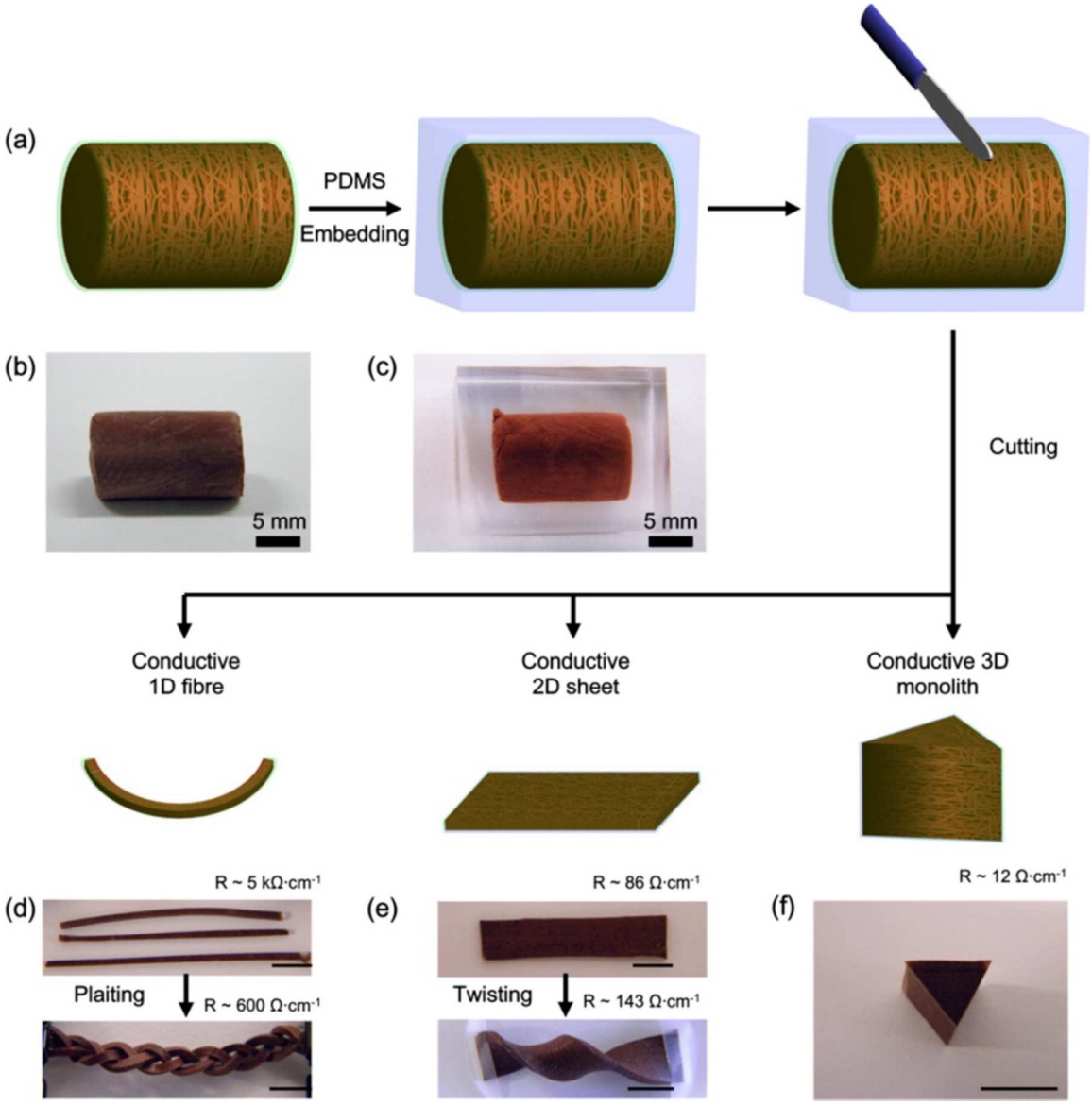

Figure 14. Manufacturability of conducting rubber ambers by simple knife cutting. a) Schematic of the amber fabrication process and the subsequent cut-shaping process. Photographic images of Cu NW-PVA aerogel monoliths (b) before and (c) after PDMS embedding. d-f) Cut-shaped 1D, 2D, and 3D structures. All of the cut-shaped rubbers were conductive and the scale bar is 1 cm. Reproduced with permission from ref. 84. Copyright 2014, American Chemical Society.

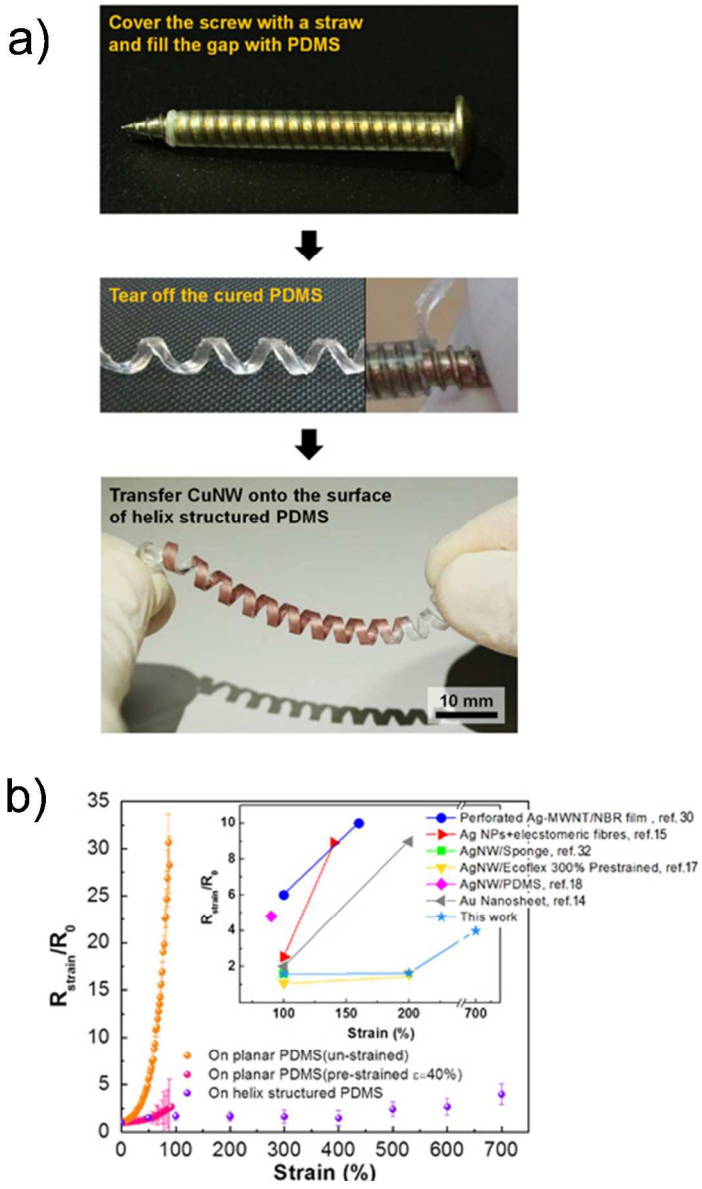

Figure 15. a) Photographs of the fabrication process for the helical-structured Cu NW electrodes. b) Relative resistance variation as a function of strain for stretchable Cu NW electrodes fabricated on both planar and helical-structured PDMS substrates. Both substrates were maintained under unstrained conditions while transferring the Cu NW network films. Reproduced with permission from ref. 85. Copyright 2014, Nature Publishing Group.